Eur Biophys J (1997) 26: 349–357

ARTICLE

M. Amrein · A. von Nahmen · M. Sieber

A scanning force- and fluorescence light microscopy study of the structure and function of a model pulmonary surfactant

Received: 20 September 1996 / Accepted: 22 May 1997

Abstract The structure of an artificial pulmonary surfactant was studied by scanning force- and fluorescence light microscopy (SFM, and FLM, respectively). The surfactant – a mixture of dipalmitoylphosphatidylcholine (DPPC), dipalmitoylphosphatidylglycerol (DPPG) and recombinant surfactant-associated protein C (SP-C) – was prepared at the air-water interface of a Langmuir film balance and imaged by FLM under various states of compression. In order to visualize their topography by SFM, the films were transferred onto a solid mica support by the Langmuir-Blodgett (LB) technique. We found that a region of high film compressibility of the spread monolayer close to its equilibrium surface pressure ($\pi = 50$ mN/m) was due to the exclusion of layered protrusions with each layer 5.5 to 6.5 nm thick. They remained associated with the monolayer and readily reinserted upon expansion of the film. Comparison with the FLM showed that the protrusions contained the protein in high concentration. The more the film was compressed, the larger was the number of layers on top of each other. The protrusions arose from regions of the monolayer with a distinct microstructure that may have been responsible for their formation. The molecular architecture of the microstructure remains to be elucidated, although some of it can be inferred from spectroscopic data in combination with the SFM topographical images. We illustrate our current understanding of the film structure with a molecular model.

Key words Scanning force microscopy · Fluorescence light microscopy · Pulmonary surfactant · Pulmonary surfactant protein C · Monolayer · Langmuir-Blodgett technique

M. Amrein
Institut für Medizinische Physik und Biophysik,
Westfälische Wilhelms-Universität,
Robert-Koch-Strasse 31, D-48149 Münster, Germany

A. von Nahmen · M. Sieber (✉)
Institut für Biochemie, Westfälische Wilhelms-Universität,
Wilhelm-Klemm-Strasse 2, D-48149 Münster, Germany

Introduction

The surface tension of the air/alveolar interface is strongly reduced by the pulmonary surfactant. It consists of a mixture of lipids and specific proteins that are secreted by the alveolar epithelial cells (Bangham et al. 1979; Brown 1964; Notter et al. 1980). Neutral phosphatidylcholines represent 80% of the surfactant mass. Among these, dipalmitoylphosphatidylcholine (DPPC) seems to play the major role in the lowering of surface tension because it is able to form stable monolayers at close-to-zero surface tension (Brown 1964; Notter et al. 1980). 5–10% of the lipids are negatively charged phosphatidylglycerols (PG) (Shelly et al. 1982). They strongly augment the adsorption of vesicular matter to the surface monolayer. In addition, there are at least four distinct surfactant-associated proteins, SP-A, SP-B, SP-C, and SP-D (e.g., Shelly et al. 1982; Possmayer 1988; Weaver 1988; Hawgood 1989; Johansson et al. 1994a) that play a decisive role with regard to the biophysical properties, the metabolism and the host defense of the pulmonary surfactant. SP-C and SP-B are highly hydrophobic proteins that are co-purified with the lipids of the surfactant upon extraction of lung lavage with organic solvents. SP-A and SP-D are hydrophilic proteins.

In the present study, we focused on the role of the surfactant-associated protein C concerning the biophysical properties of the surfactant. In particular, the interaction of the protein with the phospholipids DPPC and dipalmitoylphosphatidylglycerol (DPPG) was investigated. In the case of human surfactant, SP-C is composed of 35 amino acids (molecular mass ~4 kDa). Two palmitoyl groups are covalently linked to the two cysteine residues located in the N-terminal region. The C-terminal region (amino acids 14–35) contains almost exclusively hydrophobic amino acids. CD- as well as IR-spectroscopy revealed that the protein occurs predominantly in an α-helical secondary structure under physiological conditions (see below). The ternary structure of SP-C in an organic solvent, and in micellar solution, respectively, was solved by two-dimensional ^{1}H NMR (Johannson et al. 1994b, Johannson et al.

1995). The hydrophobic C-terminal region was a highly regular α-helix. The conformation of the hydrophilic N-terminal part as well as the conformation of the palmitoyl groups was flexibly disordered.

It was found that SP-C, together with SP-B, is responsible for the rapid adsorption and spreading of vesicular matter from the hypophase to the monolayer until the equilibrium surface pressure of about 50 mN/m is reached (Oosterlaken-Dijksterhuis et al. 1991 a – b; Pèrez-Gil et al. 1992 b; Wang et al. 1995). Post et al. (1995) and Taneva and Keough (1994 a – b) have demonstrated by means of surface balance studies that SP-C and SP-B, together with phospholipids, are excluded from the monolayer on compression above the equilibrium surface pressure. The extent of the exclusion depends on experimental parameters such as the compression rate, the initial protein concentration and even the freshness of the surface active substances (Schürch et al. 1995; Taneva and Keough 1994 a). The excluded matter reinserts into the monolayer upon expansion (Post et al. 1995; Taneva and Keough 1994 a – d).

In the lung too, the exclusion of matter from the active monolayer and the reinsertion seems to play an important role. Schürch et al. (1995) found by transmission electron microscopy of rat lung thin sections that the surfactant consisted of several layers of surface active material associated with the monolayer at the air/alveolar lining interface. It is assumed that this "surface-associated reservoir" (Schürch et al. 1995) instantaneously replenishes the active monolayer upon expansion, when otherwise the surface tension would increase. In vitro studies demonstrate that the exclusion of matter refines the active monolayer (Clements et al. 1958). The "squeeze-out" of the more fluid moieties upon repeated compression and expansion of natural surfactant allowed a surface tension near zero to be reached upon a film area reduction in the same range as is encountered for the active surface area of the lung upon breathing (max. 30%). Both, the insertion of matter into the active monolayer as well as the exclusion can progress via the cooperative movement of large units of molecules. This was observed in the pulsating bubble surfactometer and by the captive bubble technique. A sudden increase of the surface tension occurred upon cooperative exclusion; a rapid decrease of the surface tension was indicative of cooperative insertion (adsorption clicking) (Goerke and Clements 1986; Schürch et al. 1994).

In the present work, attention is directed to the structural basis of the reversible exclusion of surfactant matter out of the monolayer of a model pulmonary surfactant close to its equilibrium surface tension. Mixed films of DPPC, DPPG, and SP-C were prepared at the air/water interface of a Langmuir trough. The distribution of fluorescence labeled SP-C (NBD-SP-C), or fluorescence labeled lipid (NBD-PC), respectively, was observed by fluorescence light microscopy (FLM). Scanning force microscopy (SFM) was used to obtain the topographical structure of the film after Langmuir-Blodgett (LB) transfer to a mica support. We investigated films at various stages of compression, i. e. under conditions where no exclusion had taken place yet, and conditions where material was excluded from the monolayer. The reinsertion of the excluded matter was observed on films that were first compressed and then expanded again (the experimental procedures and statistical analysis are described in greater detail elsewhere, von Nahmen et al. 1997a, b).

Materials and methods

Surfactant

Human recombinant SP-C was a generous gift from Byk-Gulden Pharmaceuticals (Konstanz, FRG). The amino acid sequence was (GIPCCPVHLKRLLIVVVVV-VLIVVVIVGALLMGL). The two cystein residues were palmitoylated. 1,2-Dipalmitoyl-sn-Glycero-3-Phosphocholine (DPPC) and 1,2-Dipalmitoyl-sn-Glycero-3-(Phospho-rac-(1-glycerol))(DPPG) were obtained from Avanti Polar Lipids Inc. (Alabaster, AL) and used without further purification. NBD labeled SP-C (NBD-SP-C) was synthesized from SP-C and NBD-fluoride (von Nahmen et al. 1997 b). 1-Palmitoyl-2(6-((7-nitro-2-1,3-benzoxadiazo-4-yl)amino)caproyl)-sn-Glycero-3-Phosphocholine (NBD-PC) was purchased from Molecular Probes (Eugene, OR). All solvents were HPLC grade and were bought from Merck (Darmstadt, FRG). The composition chosen for all experiments followed the published results of lung lavage analysis. The amount of SP-C was 0.4 mol%, the DPPC/DPPG molar ratio was 4 : 1.

Film balance measurements

The film balance experiments were performed with a Wilhelmy balance (Riegler and Kirstein, Mainz, FRG) at 20 °C on a pure water subphase (Mili-Q185Plus, Millipore GmbH Eschborn, FRG). Monolayers were prepared by spreading aliquots of lipid/SP-C mixtures directly from a $CHCl_3/CH_3OH$ (1 : 1, vol : vol) solution onto the surface. After the solvent was allowed to evaporate for 10 minutes, the compression was started with a rate of 3 $Å^2$ per molecule and minute.

Langmuir-Blodgett transfer

For the Langmuir-Blodgett (LB) transfer, the films were prepared on a Lauda trough (Lauda-Königshofen, FRG) under the conditions described above. Prior to spreading, a fluorescence marker (see below) was added to the films. After equilibration to a well defined pressure (±1 mN/m), freshly cleaved mica sheets (Electron Microscopy Science München, FRG) were plunged through the surface at high speed (300 mm/min). The films were deposited on the upstroke (2 mm/min). We only considered samples exhibiting at least 95% transfer and showing similar fluorescence microscopical pattern before and after transfer.

Fluorescence microscopy

Fluorescence microscopy was performed using an Olympus STM5-MJS light microscope (Olympus, Hamburg, FRG). Images were taken both directly at the air/water interface and after the Langmuir-Blodgett transfer. We used either nitrobenzoxadiazol (NBD) labeled phosphatidylcholin (NBD-PC) or NBD labeled SP-C (NBD-SP-C) as the fluorescence probe. In the first case 1 mol% of all lipids were probe molecules. In the second case, all protein molecules were labelled. We observed no change in the isotherms of the lipid/protein mixtures upon the use of either of the two dyes, regardless of the fact that the addition of NBD-PC had reportedly influenced the isotherms of pure lipids (Leufgen et al. 1996).

Scanning force microscopy

SFM was performed using both a conventional microscope and a modified set-up. The conventional SFM was a Park Scientific Instrument, Autoprobe CP, used in the contact mode (i. e. with the tip in contact with the sample). The modified set-up is described elsewhere (Amrein et al. 1995). All measurements were done in air after LB transfer to mica.

Results

Surface balance measurement

On compression, the film pressure of the lipid/protein monolayer increased hyperbolically to a value of 50 to 55 mN/m (Fig. 1). On further compression, the compressibility of the film increased abruptly. This led to a plateau in the pressure/area diagram. The transition from the region of steep increase in the film pressure to the plateau region was sharply defined. In the plateau region the mean molecular area A_M varied from about 0.45 nm^2 to 0.25 nm^2, while the lower value strongly depended on the compression rate. At the end of the plateau, the compressibility decreased again sharply. Repeated compression-expansion cycles led to isotherms shifted slightly to lower molecular areas, if compression was stopped at the end of the plateau region at the latest. The slight shift was ascribed to continued equilibration processes in the film during the period of the experiment. On compression to mean molecular areas A_M lower than 0.25 nm^2 the film pressure rose again. Under those conditions, repeated compression-expansion cycles led to isotherms shifted successively to lower molecular areas after each expansion of the film. These shifts may be explained by a loss of material into the subphase or the formation of collapse structures unable to respread on expansion.

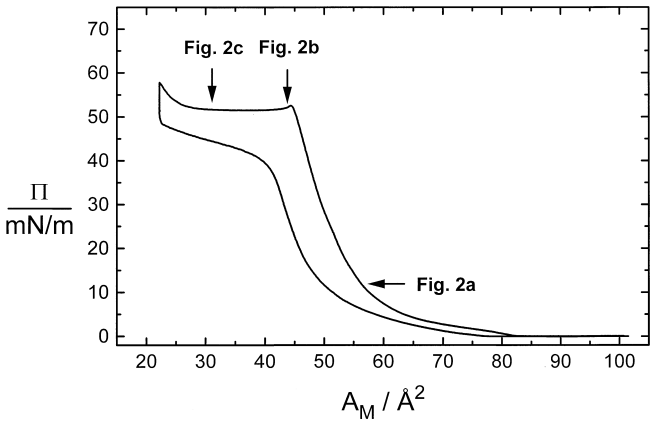

Fig. 1 Pressure-area diagram of a mixed DPPC/DPPG/SP-C film. The lipid molar ratio is 4:1. The film contains 0.4 mol% protein. The first compression with following expansion are shown. *Arrows* point to three states of the film where the images shown in Fig. 2 were taken

FLM of mixed films

In the early stage of compression of a mixed film containing fluorescence labeled phosphatidylcholine (NBD-PC), the formation of two domains was observed (Fig. 2 a). There was a dark domain that formed disks with a diameter of several micrometers. The disks were embedded in a bright domain.

We used statistical methods (Nahmen et al. 1997 b) to evaluate mean intensities and areas of the domains. For that purpose histograms were calculated from the images. Fitting the sum of two Gaussian's to the histograms gave the values of the mean fluorescence intensities of the bright domain, $\overline{I_b}$ and the dark domain, $\overline{I_d}$, and also the areas A_L and A_D, covered by the two different domains.

Upon further compression, the overall area A_d of the dark domain increased. This behavior led to the conclusion that the dark domain was a liquid condensed (lc) phase of pure phospholipids. Labeled lipids as well as SP-C were excluded from this phase. This assumption was verified by an experiment where the protein was labeled directly (Nahmen et al. 1997a). Most probably, besides of proteins, the bright domain contained lipids that were in a liquid expanded (le) state.

Above a film pressure of 10 mN/m, the fluorescence intensity of the bright domain decreased upon compression and an extremely low contrast between the domains resulted. This is explained by self quenching of the dye molecules due to the enrichment in the bright domain. An increasing alignment to each other resulting in strong dipole-dipole interactions may result in the low fluorescence intensity.

In contrast, in the plateau region of the pressure area diagram (between $A_M = 0.25$ nm^2 and $A_M = 0.45$ nm^2) the mean intensity $\overline{I_b}$ of the bright domain increased linearly with decreasing molecular area, whereas the mean intensity $\overline{I_d}$ of the dark domain remained constant. Therefore, the contrast between the domains increased strongly until the end of the plateau was reached (compare Fig. 2 b and

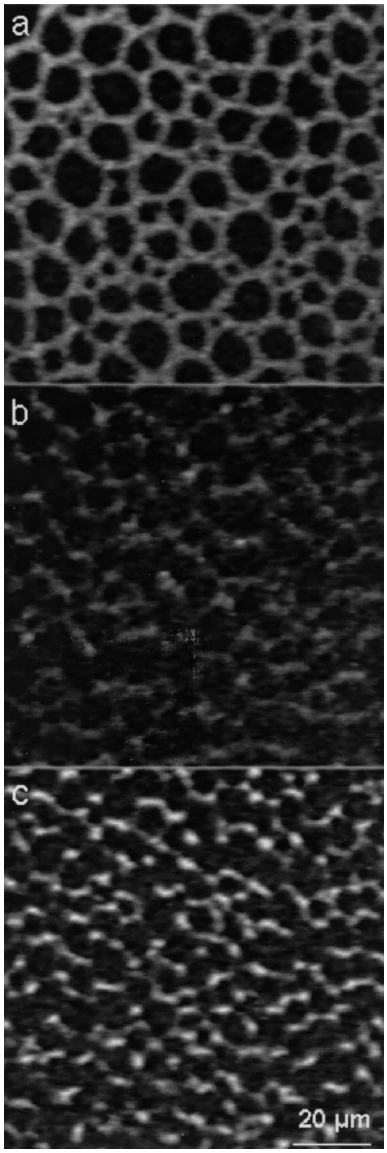

Fig. 2a–c Fluorescence light microscopical images of a mixed DPPC/DPPG/SP-C film token at different stages of compression. The physical states of the film are marked in Fig. 1

Fig. 2c). This can be accounted for by the formation of three-dimensional structures of the dye containing matter associated with the monolayer. The intensity increase is then due to the higher amount of dye molecules in the focal plane. The whole process could be reversed by expanding the film.

SFM images of the LB-films

The SFM images of films transferred from the air-water interface to mica at a pressure of 30 mN/m exhibited smooth, polygonal patches. They had a diameter of several micrometers and covered most of the sample area. Their size and shape was indicative of the fact that they coincided with the dark lipid phase of the FLM micrographs. The lipid patches were connected by a corrugated interspace. Figure 3a shows the border of the lipid phase to the corrugated interspace. Fissures divided the surface into smooth patches, 100 to 200 nm in diameter. They were often hexagonal, with an indentation in the middle. Deeper in the lipid patches, the polygons became open structures that finally disappeared. In addition, there were areas where a mesh of filaments became obvious (Fig. 3a, bottom). Figure 3b shows that these filaments were ordered in parallel, about 10 to 20 nm apart. Their diameter varied regularly along the axis, which gave them a helical appearance. In some regions the arrays of filaments were easily

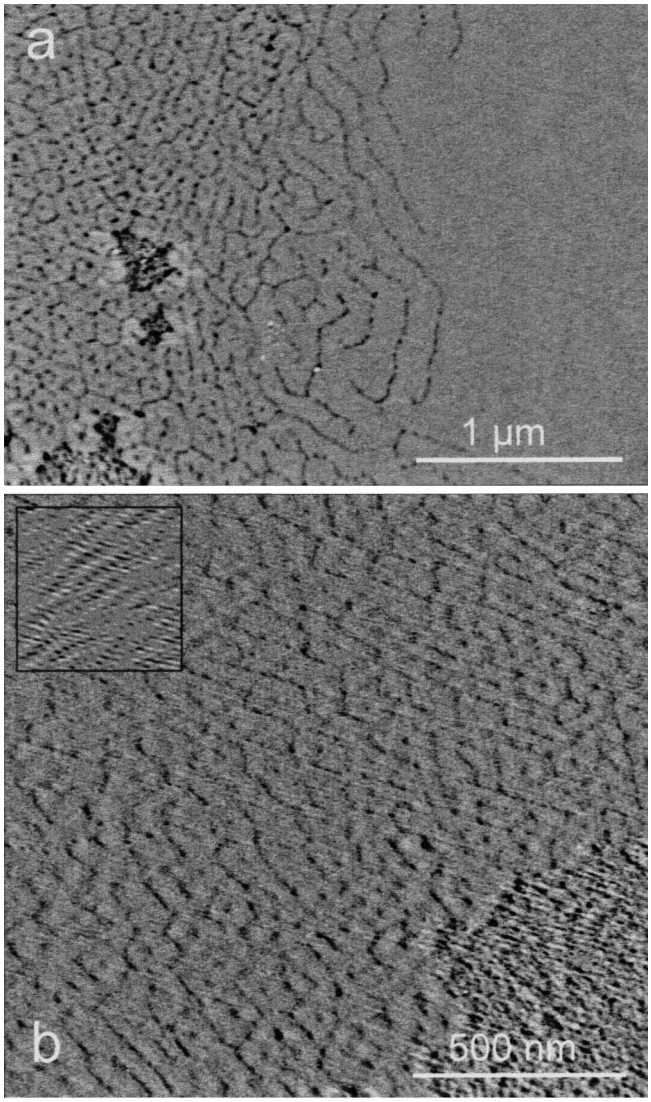

Fig. 3 SFM topography of a film at the mica-air interface, transferred below the plateau region of the pressure-area diagram (**a**). The image shows the border of a lipid patch (*right*) facing towards the protein-rich interspace (*left*). The region shown in panel (**b**) harbors both polygonal patches and a mesh of filaments (*bottom right*). Note that the filaments are still slightly visible in the region covered by polygons (*upper left*). The fourier filtered image of this area reveals the filaments more clearly (*inset*)

discernible. In the region of the small polygons they were also present, although less well visible. Their order gave rise to weak reflexes in the fourier transforms of the corresponding areas, and the inverse transform of just the reflexes revealed the filaments more clearly (Fig. 3b; inset). The fissures that framed the small hexagons were in the direction of the filaments.

The areas covered by filaments coincided with the bright regions in the FLM and, hence, contained all the SP-C and phospholipids. Consistently, when a film had a higher proportion of protein, a larger fraction of the area was corrugated.

Films that were transferred at a pressure above 50 mN/m (i.e. in the plateau of the area-pressure diagram) showed planar protrusions in the corrugated area. The level lipid patches remained unchanged. When a film was transferred at the onset of the plateau region, there were only a few small and often round protrusions. When the films were further compressed before transfer, the lateral extension of the protrusions increased and smaller protrusions appeared on top of larger ones (Fig. 4). Each layer was 5.5 to 6.5 nm thick. Furthermore, the area where protrusions were present became more confined; i. e. surfactant matter was increasingly moved from the monolayer into multilamellar protrusions. This process was reversible. When a film was first compressed to the end of the high compressibility region and then expanded, the protrusions had disappeared again.

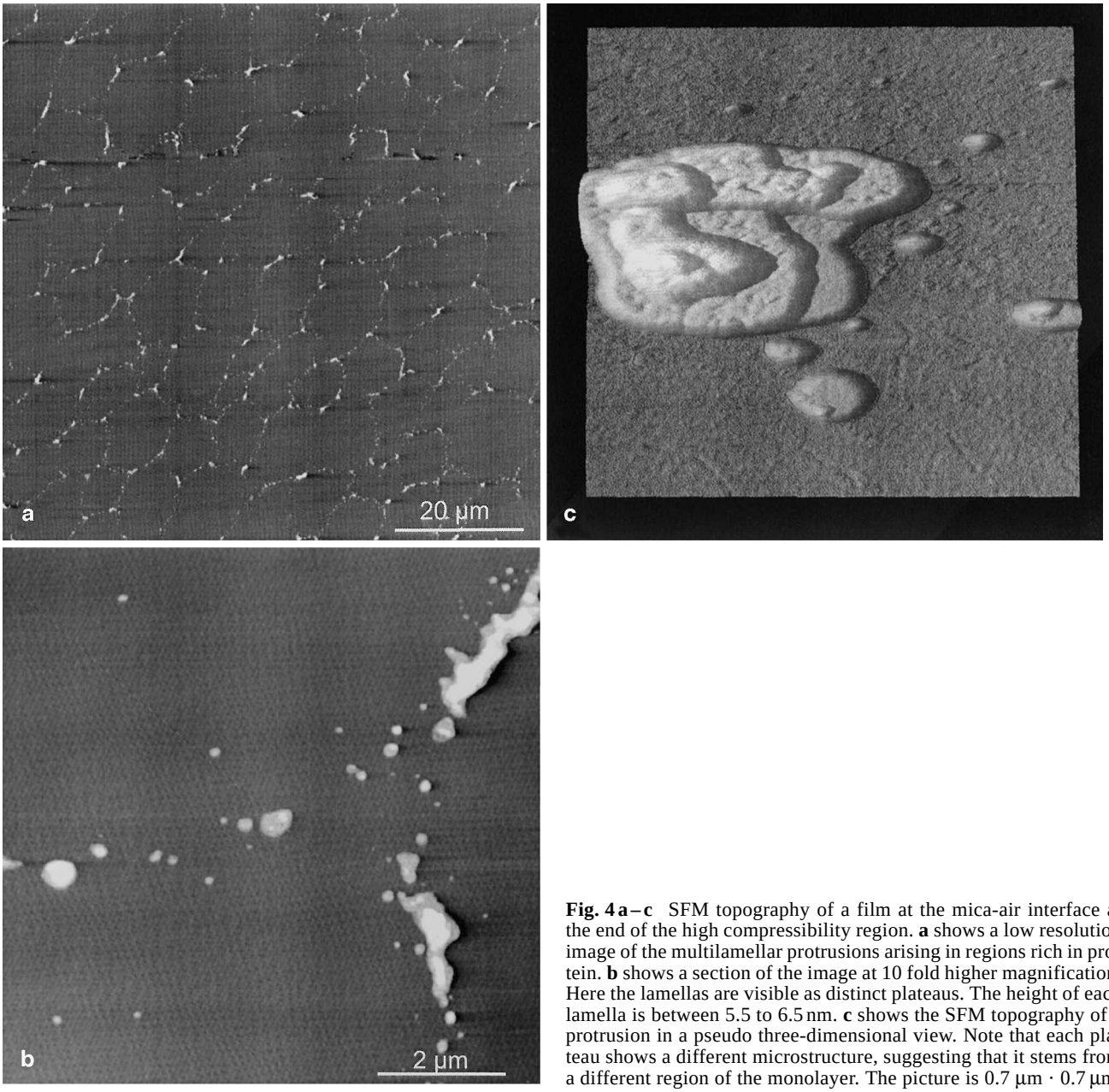

Fig. 4a–c SFM topography of a film at the mica-air interface at the end of the high compressibility region. **a** shows a low resolution image of the multilamellar protrusions arising in regions rich in protein. **b** shows a section of the image at 10 fold higher magnification. Here the lamellas are visible as distinct plateaus. The height of each lamella is between 5.5 to 6.5 nm. **c** shows the SFM topography of a protrusion in a pseudo three-dimensional view. Note that each plateau shows a different microstructure, suggesting that it stems from a different region of the monolayer. The picture is 0.7 µm · 0.7 µm

Discussion

The lipids in the smooth patches of the mixed monolayers observed at a film pressure of 30 mN/m are in the liquid-condensed (lc) state under the conditions considered in this study. It is assumed that they contain no protein, since these patches emitted no fluorescence light in the FLM, independent of the dye used. By secondary ion mass spectroscopy (SIMS) on solid supported lipid monolayers it was recently shown that lipid dyes were totally excluded from the lc phase (Leufgen et al. 1996). Most probably, this is also true for other bulky molecules such as proteins.

The lc patches are connected by a mixed lipid-SP-C interspace whose molecular architecture is much less obvious. It contains lipids and all the protein. Interestingly, the maximum height of both the pure lipid phase and the mixed interspace was mostly identical. The length of the lipid molecules, in a similar state as in the pure lipid phase, may therefore have been responsible for the thickness of the mixed phase. In order to understand how the SP-C molecules are accommodated in the monolayer, their conformation and orientation in monolayers of the protein may be considered. Here, they are mainly α-helical (~60%) aside from a smaller amount of random coild (~40%). The helical axis is close-to-parallel to the air-water interface (Creuwels et al. 1993). The α-helical content is also predominant, when the SP-C interacts with lipids (see below). We therefore assume that in the lipid-protein mixed monolayers, the SP-C exhibits a similar secondary structure and orientation, although there is no direct experimental evidence. With this assumption, they are not able to span the monolayer perpendicularly, because their length is almost twice the thickness of the monolayer. Lavigne et al. (1992) suggested that pure hydrophobic α-helices at the air-water interface could adopt a higher order helical structure at a surface pressure similar to that applied in the present study. Such films become ordered upon compression (Malcolm 1973). Consistently, we found that a seemingly filamentous, ordered structure was responsible for the observed SFM topographies. There even seemed to be two or three such arrays on top of each other. Hence, a mesh of higher order helical protein filaments parallel to the air-water interface could have formed the core of such regions of the monolayer. The spacing between the filaments could have been filled up by lipid molecules that spanned the monolayer perpendicular to the film plane. The SFM topographies suggest that the density of the lipids increased towards the pure lipid phase. The fissures that framed the small polygons seen in most part of these regions may have been caused by a molecular misfit within this lipid-protein complex structure.

When a pure lipid film at the air-water interface is compressed beyond a certain surface pressure, it collapses irreversibly. Then, the film pressure no longer rises on compression. Instead, the film pressure course shows a wiggly shape on further compression. Upon expansion, the film pressure decreases immediately because the collapsed film cannot spread at the interface anymore. In contrast, the SP-C-lipid mixed film exhibited a stable, constant film pressure in the collapse region leading to a plateau in the pressure-area diagram. On expansion, the excluded matter respreads into the monolayer. What we want to know is the structural basis of this unique property.

The SFM- as well as the FLM images show that an increasing amount of the monolayer matter accumulated in lamellar protrusions when the film was compressed within the plateau region of the pressure-area diagram. These protrusions disappeared again when the film was expanded. The height of a single lamella varied between 5.5 to 6.5 nm. This is 0.5 to 1.5 nm more than the height h of a DPPC double layer as measured with the SFM under similar conditions (h_{DPPC}~5 nm, data not shown). Nevertheless, we assume that the protrusions are based on integer multiples of a lipid double layer. Taking this assumption into account, the area of the monolayer lost through compression was correctly found by summing up the total area of all protrusion layers. The larger height compared to a lipid double layer may be due to the included proteins. Tchoreloff et al. (1991) found similar structures in LB films of lung surfactant extract films by transmission electron microscopy. They, too, interpreted the protrusions as stacks of lipid bilayers.

Unfortunately, the SFM images do not reveal directly whether the protrusions formed towards the air or the aqueous subphase. The two possibilities are depicted in Fig. 5. They are based on the assumption that the protrusions were in fact based on lipid double layers. If they formed to the air (a), the double layers on top of the monolayer would have been in a reversed conformation; i. e., with the hydrophilic head groups oriented to the interior. The LB transfer to the solid support would then leave the protrusions directly accessible to the SFM tip with the topmost layer exposing the hydrophobic acyl chains. If the protrusions were towards the aqueous subphase (b), however, they would have become locked between the monolayer and the mica support upon LB transfer. The SFM would then have imaged the monolayer covering the protrusions, rather than the topography of the protrusions themselves.

The shape of the protrusions suggests that many small, round patches were squeezed out. In some cases, the smallest entities excluded seemed to coincide with the small polygonal patches seen in the films at $\pi = 30$ mN/m. On further compression the protrusions then probably grew in size and coalesced into the larger structures. There also arose small protrusions on top of larger ones. We observed piles with up to 10 equidistant steps within those regions. The formation of the multilamellar structures could have been a mere folding of the monolayer and the molecular structure would not have changed. It just as well could have progressed via the “budding” of surfactant matter, induced by the specific monolayer structure. The lipids and the protein could then have rearranged completely.

At the air-water interface of a Langmuir trough the protrusions are inhomogeneously distributed across the interface. There is good reason to suppose that the inhomogeneous distribution is due to the preparation technique: Protrusions can only form in the regions of the former liquid

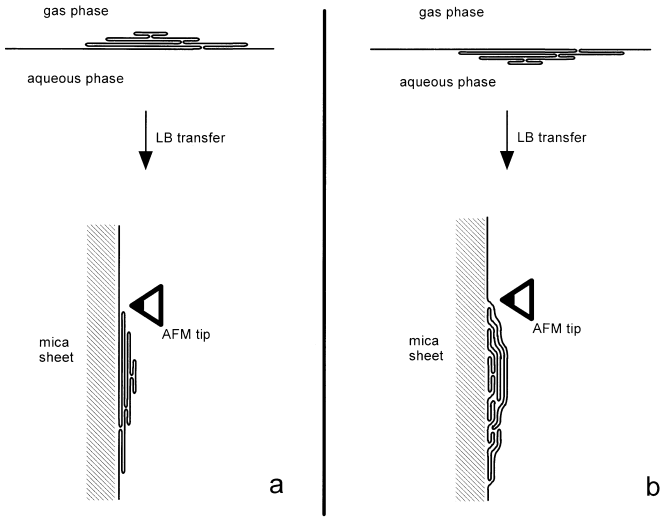

Fig. 5 Two possible orientations (**a, b**) of the protrusions at the air-water interface and after Langmuir-Blodgett transfer to mica

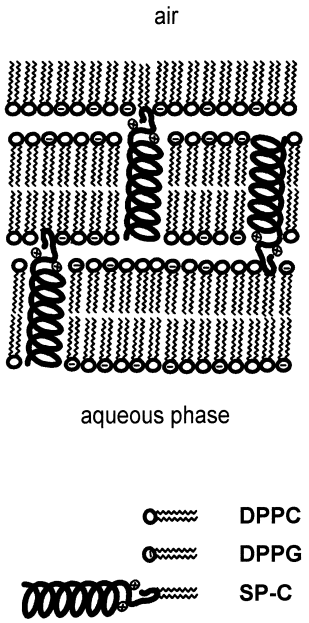

Fig. 6 Molecular model of the protrusions

expanded phase of the monolayer which is rich in protein. In contrast, at the air/alveolar interface of the lung surfactant material spreads continuously from vesicular structures of the subphase. Therefore, the protrusions may form a nearly homogeneous multilayer adjacent to the surface. Such kinds of multilayers were in fact observed by electron microscopy in rabbit lungs fixed by vascular perfusion (Schürch et al. 1995).

As in the case of the monolayer, the molecular structure of the protrusions was not directly revealed by SFM. In an attempt to understand the possible arrangement of SP-C in the protrusion, we consider spectroscopic data of mixed lipid-protein vesicles. Vesicles are the structures most closely related to the protrusions. Fourier transform infrared (FT-IR) spectroscopy of SP-C incorporated in phospholipid vesicles revealed a predominantly α-helical secondary structure (60 to 90%) with the helix axis almost parallel to the lipid acyl chains (Pastrana et al. 1991; Vandenbussche et al. 1992; Clercx et al. 1995). Palmitoylated SP-C exhibited an increased α-helix content. It is assumed that the α-helical moiety of SP-C spans the lipid bilayers in vesicles and the remaining moiety interacts with the lipid head groups (Post et al. 1995; Johansson et al. 1995). This assumption is obvious considering some characteristics of the molecular structure of SP-C: Starting from the carboxy terminus, most of the protein forms a highly hydrophobic α-helix (amino acids 9 to 34), ~37 Å in length, in the case of the published NMR structure of porcine SP-C (Johansson et al. 1994b; Johannsson et al. 1995). It allows for hydrophobic interaction with the interior hydrophobic part of the bilayer. The histidine, lysine, and arginine (positions 9, 11, and 12 of the human sequence) are hydrophilic, with the lysine and arginine positively charged at physiological pH. The electrostatic interactions between these charged residues and the negatively charged DPPG may further stabilize the structure. This is supported by calorimetric studies on vesicles that revealed the ability of SP-C to withdraw PG from phase separated PG/PC mixtures (Post et al. 1995).

The two cysteines are acylated with two palmitic acids. This post-translational modification is highly preserved in evolution and, hence, may play an important functional role. However, the orientation of the palmitoyl groups in the multilamellar structures is not clear at all. One possible orientation is depicted in Fig. 6.

Conclusions

A mixture of three lung surfactant components spread at the air/water interface was able to mimic some of the main biophysical properties of the surface film present at the air/alveolar interface. A high surface coverage with DPPC monolayer patches was responsible for the low surface tension of about 20 mN/m. In order to keep the low surface tension during surface area changes, surfactant matter was stored in a surface associated reservoir. On expansion (inhalation) the surface active matter spread from this reservoir into the monolayer and vice versa. The reservoir was organized in the form of stacks of bilayers enriched in non-DPPC compounds. According to the molecular model worked out, the multilamellar structures were stabilized by the SP-C molecules incorporated with their hydrophobic α-helix in one bilayer and stretching their palmitoyl groups into a neighboring bilayer, or the surface active monolayer, respectively (Fig. 6). In the monolayer, there was a distinct lipid-protein complex structure that was seemingly responsible for the formation of the multilamellar protrusions.

In vivo too, such a surface-associated reservoir is present: Schürch et al. (1995) observed by electron microscopy multilamellar structures in thin sections of rabbit

lungs, fixed by vascular perfusion. This reservoir may continously be filled up by vesicles of surfactant from the aqueous hypophase, thus compensating for a loss of surfactant material due to uptake by macrophages and type II alveolar epithelia cells or draining off into bronchiole, respectively.

In the present work we have drawn attention to the role of the SP-C in the formation of a surface-associated reservoir. It has to be pointed out that other compounds of the lung surfactant will, of course, also contribute to the biophysical properties of the surface film in vivo. As found by others (Oosterlaken-Dijksterhuis et al. 1992) SP-B enhances the spreading of vesicles to the surface film – a property not analyzed in the present publication. The diversity of other lipid components – especially unsaturated ones – may enhance the reorientation processes inside the surface associated reservoir.

Although we have emphasized our current understanding of the surface associated reservoir by a molecular model of the film structure, the microscopical basis is by no means sufficient to draw definite conclusions. The structural investigation may have to be supplemented by additional techniques, such as transmission electron microscopy. Future work will also have to include those components of the lung surfactant omitted in the present study.

Acknowledgements We thank R. Reichelt and H.-J. Galla for very valuable discussions and continued support and L. Melanson for careful English corrections. This work was supported by grants No. Re 782/2-1 (to R. R. and M. A.) awarded by the Deutsche Forschungsgemeinschaft and No. IV A 6-400 005 91 (to R. R.) awarded by the Ministerium für Wissenschaft und Forschung des Landes Nordrhein-Westfalen. The generous support by Byk Gulden Pharmaceuticals, who supplied us with the recombinant SP-C, is gratefully acknowledged.

References

Amrein M, Schenk M, von Nahmen A, Sieber M, Reichelt R (1995) A novel force-sensing arrangement for combined scanning force/scanning tunnelling microscopy applied to biological objects. J Microscopy 179: 261 – 265

Bangham AD, Morley CJ, Phillips MC (1979) The physical properties of an effective lung surfactant. Biochimica et Biophysica Acta 573: 552 – 556

Brown ES (1964) Isolation and assay of dipalmitoyl lecithin in lung extracts. Am J Physiol 207: 402 – 406

Clements JA, Brown ES, Johnson RP (1958) Pulmonary surface tension and the mucous lining of the lungs: some theoretical considerations. J Appl Physiol 12: 262 – 268

Clercx A, Vanderbussche G, Curstedt T, Johansson J, Jörnvall H, Ruysschaert J-M (1995) Structural and functional importance of the C-terminal part of the pulmonary surfactant polypeptide SP-C. Eur J Biochem 229: 465 – 472

Creuwels LAJ, Demel RA, van Golde LMG, Benson BJ, Haagsman HP (1993) Effect of acylation on structure and function of surfactant protein C at the air-liquid interface. J Biol Chem 268: 26 752 – 26 758

Goerke J, Clements JA (1986) Alveolar surface tension and lung surfactant. In: Fishman AP et al. (eds) Handbook of Physiology, Section 3: The respiratory system, vol III, Part 1. American Physiological Society, Bethesda, MD, pp 247 – 261

Hawgood S (1989) Pulmonary surfactant apoproteins: a review of protein and genomic structure. Am J Physiol 1: 13 – 22

Johansson J, Cursted T, Robertson B (1994 a) The proteins of the surfactant system. Eur Respir J 7: 372 – 391

Johansson J, Szyperski T, Curstedt T, Wüthrich K (1994 b) The NMR structure of the pulmonary surfactant-associated polypeptide SP-C in an apolar solvent contains a valyl-rich α-helix. Biochemistry 33: 6015 – 6023

Johansson J, Szyperski T, Wüthrich K (1995) Pulmonary surfactant-associated polypeptide SP-C in lipid micelles: CD studies of intact SP-C and NMR secondary structure determination of depalmitoyl-SP-C (1 – 17). FEBS Lett 362: 261 – 265

Lavigne T, Tancrède P, Lamarche F, Max J-J (1992) Packing of hydrophobic α-helices: a study at the air/water interface. Langmuir 8: 1988 – 1993

Leufgen KM, Rulle H, Benninghoven A, Sieber M, Galla H-J (1996) Imaging time-of-flight secondary ion mass spectrometry allows visualization and analysis of coexisting phases in Langmuir-Blodgett films. Langmuir 12: 1708 – 1711

Malcolm BR (1973) The structure and properties of monolayers of synthetic polypeptides at the air-water interface. Prog Surf Membr Sci 7: 183 – 229

Nahmen A von, Schenk M, Sieber M, Amrein M (1997a) The structure of a model pulmonary surfactant as revealed by scanning force microscopy. Biophys J 72: 463 – 469

Nahmen A von, Post A, Galla H-J, Sieber M (1997b) The phase behaviour of lipid monolayers containing pulmonary surfactant protein C studied by fluorescence light microscopy. Eur Biophys J 26: 359 – 369

Notter RH, Tabak SA, Mavis RD (1980) Surface properties of binary mixtures of some pulmonary surfactant components. J Lipid Res 21: 10 – 22

Oosterlaken-Dijksterhuis MA, Haagsman HP, van Golde LMG, Demel RA (1991 a) Characterisation of lipid insertion into monomolecular layers mediated by lung surfactant proteins SP-B and SP-C. Biochemistry 30: 10 965 – 10 971

Oosterlaken-Dijksterhuis MA, Haagsman HP, van Golde LMG, Demel RA (1991 b) Interaction of lipid vesicles with monomolecular layers containing lung surfactant proteins SP-B or SP-C. Biochemistry 30: 8276 – 8281

Oosterlaken-Dijksterhuis MA, van Eijk M, van Golde LMG, Haagsman HP (1992) Lipid mixing is mediated by the hydrophobic surfactant protein SP-B but not by SP-C. Biochim Biophys Acta 1110: 45 – 50

Pastrana B, Mautone AJ, Mendelsohn R (1991) Fourier transform infrared studies of secondary structure and orientation of pulmonary surfactant SP-C and its effect on the dynamic surface properties of phospholipids. Biochemistry 30: 10 058 – 10 064

Pattle RE (1958) Properties, function and origin of the alveolar lining layer. Proc R Soc Lond 148: 217 – 240

Pauls KP, MacKay AL, Bloom M (1983) Deuterium nuclear magnetic resonance study of the effects of palmitic acid on dipalmitoylphosphatidylcholine bilayers. Biochemistry 22: 6101 – 6109

Pèrez-Gil J, Nag K, Taneva S, Keough KMW (1992 a) Pulmonary surfactant protein SP-C causes packing rearrangements of dipalmitoylphosphatidylcholine in spread monolayers. Biophys J 63: 197 – 204

Pèrez-Gil J, Tucker J, Simatos G (1992 b) Interfacial adsorption of simple lipid mixtures combined with hydrophobic surfactant protein from pig lung. Biochem Cell Biol 70: 332 – 338

Pèrez-Gil J, López-Lacomba JL, Cruz A, Beldarraín A, Casals C (1994) Deacylated pulmonary surfactant protein SP-C has different effects on the thermotropic behaviour of bilayers of dipalmitoylphosphatidylglycerol (DPPG) than the native protein. Biochem Soc Trans 22: 372S

Possmayer F (1988) A proposed nomenclature for pulmonary surfactant-associated proteins. Am Rev Respir Dis 138: 990 – 998

Post A, von Nahmen A, Schmitt A, Ruths J, Riegler H, Sieber M, Galla H-J (1995) Pulmonary surfactant protein C containing lipid films at the air-water interface as a model for the surface of lung alveoli. Mol Membrane Biol 12: 93 – 99

Qanbar R, Possmayer F (1995) On the surface activity of surfactant-associated protein C (SP-C): effects of palmitoylation and pH. Biochim Biophys Acta 1255: 251 – 259

Schürch S (1982) Surface tension at low lung volumes: Dependence on time and alveolar size. Respir Physiol 48: 339–355

Schürch S, Schürch D, Curstedt T, Robertson B (1994) Surface activity of lipid extract surfactant in relation to film area compression and collapse. J Appl Physiol 77: 974–986

Schürch S, Qanbar R, Bachofen H, Possmayer F (1995) The Surface-Associated Surfactant Reservoir in the Alveolar Lining. Biol Neonate 67 [Suppl 1]: 61–76

Shelly SA, Balis JU, Paciga JE, Espinoza CG, Richman AV (1982) Biochemical composition of adult human lung surfactant. Lung 160: 195–206

Shiffer K, Hawgood S, Haagsman HP, Benson B, Clements JA, Goerke J (1993) Lung surfactant proteins, SP-B and SP-C, alter the thermodynamic properties of phospholipid membranes: a differential calorimetry study. Biochemistry 32: 590–597

Taneva SG, Keough KMW (1994a) Dynamic surface properties of pulmonary surfactant proteins SP-B and SP-C and their mixtures with dipalmitoylphosphatidylcholine. Biochemistry 33: 14660–14670

Taneva SG, Keough KMW (1994b) Pulmonary surfactant proteins SP-B and SP-C in spread monolayers at the air-water interface: I. Monolayers of pulmonary surfactant protein SP-B and phospholipids. Biophys J 66: 1137–1148

Taneva SG, Keough KMW (1994c) Pulmonary surfactant proteins SP-B and SP-C in spread monolayers at the air-water interface: II. Monolayers of pulmonary surfactant protein SP-C and phospholipids. Biophys J 66: 1149–1157

Taneva SG, Keough KMW (1994d) Pulmonary surfactant proteins SP-B and SP-C in spread monolayers at the air-water interface: III. Proteins SP-B plus SP-C with phospholipids in spread monolayers. Biophys J 66: 1158–1166

Tchoreloff P, Gulik A, Denizot B, Proust JE, Puisieux F (1991) A structural study of interfacial phospholipid and lung surfactant layers by transmission electron microscopy after Blodgett sampling: influence of surface pressure and temperature. Chem Physics Lipids 59: 151–165

Vandenbussche G, Clercx A, Clercx M, Curstedt T, Johansson J, Jörnvall H, Ruysschaert J-M (1992) Secondary structure and orientation of the surfactant protein SP-B in a lipid environment. A fourier transform infrared spectroscopy study. Biochemistry 31: 9169–9176

Wang Z, Hall SB, Notter RH (1995) Dynamic surface activity of films of lung surfactant phospholipids, hydrophobic proteins, and neutral lipids. J Lipid Res 36: 1283–1293

Weaver TE (1988) Pulmonary surfactant-associated proteins. Gen Pharmacol 19: 361–368